Available online at www.sciencedirect.com
ScienceDirect
Biochimica et Biophysica Acta 1767 (2007) 1180–1188
Biochimica et Biophysica Acta BBA
www.elsevier.com/locate/bbabio

Structural and functional self-organization of Photosystem II in grana thylakoids

Helmut Kirchhoff [a,*], Winfried Haase [b], Silvia Haferkamp [a], Thomas Schott [c], Mauricio Borinski [a], Ulrich Kubitscheck [d], Matthias Rögner [c]

[a] *Institut für Botanik, Schlossgarten 3, D-48149 Münster, Germany*
[b] *Max-Planck-Institut für Biophysik, Max-von-Laue-Str. 3, D-60438 Frankfurt am Main, Germany*
[c] *Lehrstuhl für Biochemie der Pflanzen, Ruhr Universität, D-44780 Bochum, Germany*
[d] *Institut für Physikalische und Theoretische Chemie, Wegelerstrasse 12, D-53115 Bonn, Germany*

Received 10 May 2007; accepted 31 May 2007
Available online 8 June 2007

Abstract

The biogenesis of the well-ordered macromolecular protein arrangement of photosystem (PS)II and light harvesting complex (LHC)II in grana thylakoid membranes is poorly understood and elusive. In this study we examine the capability of self organization of this arrangement by comparing the PSII distribution and antenna organization in isolated untreated stacked thylakoids with restacked membranes after unstacking. The PS II distribution was deduced from freeze-fracture electron microscopy. Furthermore, changes in the antenna organization and in the oligomerization state of photosystem II were monitored by chlorophyll *a* fluorescence parameters and size analysis of exoplasmatic fracture face particles. Low-salt induced unstacking leads to a randomization and intermixing of the protein complexes. In contrast, macromolecular PSII arrangement as well as antenna organization in thylakoids after restacking by restoring the original solvent composition is virtually identical to stacked control membranes. This indicates that the supramolecular protein arrangement in grana thylakoids is a self-organized process.

Keywords: Grana thylakoid; PSII; Repair cycle; Stacking

1. Introduction

In higher plants the photosynthetic machinery is localized in the thylakoid membrane inside the chloroplasts. A unique feature of this membrane is the formation of stacked grana thylakoids, which are interconnected by unstacked stroma lamellae; for a recent model see [1]. The spatial subcompartmentation in stacked and unstacked membrane regions forms the structural basis for a pronounced lateral segregation of the six main protein complexes involved in photosynthetic energy transduction, i.e. PSI, PSII, cyt. b/f complex, LHCI, LHCII and ATPase [2]. The main fraction of photosystem II and light harvesting complex II are concentrated in the stacked grana core, whereas PSI (with LHCI), a minor fraction of PSII and the ATPase are mainly localized in grana margins, end membranes and stroma lamellae. It is assumed that the cytochrom b/f complex is equally distributed [2]. Recently a more detailed picture about the photosystem organization emerges [3]. There is evidence that both PSI and PSII are not homogeneous but form subspecies so-called PSIIα and PSIα as well as PSIIβ and PSIβ centers. In case of PSII this may reflect intermediates during its high turnover [4]. All photosynthetic proteins are evolutionary optimized for special functions and have a complex structure which holds in particular for PSII in stacked grana regions with more than 27 subunits and more than 100

Abbreviations: Chl, chlorophyll; DCMU, 3-(3′,4′-dichlorophenyl)-1,1-dimethylurea; cyt, cytochrom; EDTA, ethylenediaminetetraacetic acid; EF, exoplasmatic fracture face; Fo, chlorophyll a fluorescence level with oxidized QA; Fm, fluorescence level with completely reduced QA; HEPES, N-2-hydroxyethylpiperazine-*N*′-2-ethane-sulfonic acid; LHC, light harvesting complex; NNDF, next neighbor distribution function; PCF, pair correlation function; PF, protoplasmatic fracture face; PS, photosystem; QA, primary quinone acceptor of photosystem II; RC, reaction center; rs, restacked; s, stacked; us, unstacked

* Corresponding author. Tel.: +49 251 8324820; fax: +49 251 8323823.
E-mail address: kirchhh@uni-muenster.de (H. Kirchhoff).

0005-2728/$ - see front matter © 2007 Elsevier B.V. All rights reserved.
doi:10.1016/j.bbabio.2007.05.009

cofactors per reaction center [5]. The PSII reaction center contains the D1, D2 and Cyt b559 subunits which bind all electron transfer cofactors. The light harvesting system of PSII consists of the core antenna complexes CP43 and CP47 (reaction center plus core antenna are named PSII-core) and light harvesting complexes. The latter are divided into the minor LHCII (CP24, CP26 and CP29) which are monomeric, and the major LHCII which are trimers. Most likely, PSII in stacked grana thylakoids is mainly organized as a so-called PSII–LHCII supercomplex [6,7] which is a core-dimer with minor LHCIIs and two major LHCII trimers. There is also evidence for additional specific weaker binding sites for LHCII-trimers on the PSII–LHCII supercomplex [6]. On average, the complete functional PSII in grana membranes is associated with about four trimeric LHCII resulting in an apparent antenna size of roughly 230 chlorophylls [5]. A more detailed investigation of the structural organization of a whole grana disc yielded evidence for a supramolecular network of LHCII and PSII complexes [8]; this was concluded from the observation that the arrangement of PSII in grana thylakoids is different from a pure random distribution indicating the presence of ordering forces.

Although the protein organization in grana thylakoids is rather complex, this arrangement is highly dynamic, which is a prerequisite for adaptations on an ever changing environment (e.g. light intensities). Especially the D1 subunit of PSII in grana stacks has a high turnover rate which causes a constant disassembling and reassembling of the whole supercomplex [9,10]. The high turnover is due to the fact that PSII is operating at very positive redox potentials causing an intrinsically high probability for photoinhibition [11]. This highlights the importance of understanding the biogenesis and turnover of protein complexes to maintain the integrity of the photosynthetic machinery. The complex reaction pathway starting from the photodamaged PSII to a functionally regenerated protein is called repair cycle and the subject of intensive research [9]. Although most recently a five-step reaction scheme for the PSII biogenesis up to the level of PSII-core monomers was proposed [4], the assembly of the PSII and LHCII network of a whole grana disc remains elusive.

One way to examine assembly/disassembly processes is to study PSII arrangements in stacked, unstacked and restacked thylakoids by electron microscopy of freeze-fractured membranes [12]. In freeze fracture the membrane is split at the hydrophobic core producing two half-membranes of which the newly generated surfaces are called protoplasmic fracture face (PF, and exoplasmic fracture face (EF). There is good evidence that PSII is exclusively localized in the EF half-membrane [12] which opens up the possibility to study its distribution [8]. Moreover, the unstacking of grana can be induced by incubation of isolated thylakoids in buffers with low ionic strength; this process is accompanied by an intermixing and randomization of the well-ordered membrane protein arrangement [12]. Starting from unstacked membranes, re-addition of cations (mainly Mg^{2+}) triggers the restacking. Comparing the PSII arrangement between untreated stacked control thylakoids and restacked membranes opens up the possibility to analyze whether the membrane has the capability for a self-organization of the LHCII–PSII network in grana discs.

In this study we examine structurally and functionally the reassembly of the LHCII–PSII arrangement in grana thylakoids by restacking of unstacked thylakoids. Mathematical methods like next neighbor distribution analysis (NNDF) and pair correlation functions (PCF) [8] enable objective comparison and quantification of PSII distribution in the EF fracture face [13]. These structural data are complemented by EF particle size analysis and also by functional investigations, which yield information on the PSIIα/PSIIβ heterogeneity [14]. Chlorophyll *a* fluorescence induction measurements are able to distinguish between PSIIα, which most likely form the LHCII–PSII supercomplex in stacked grana, and monomeric PSIIβ, with a two- to three-fold smaller antenna size. While PSIIα is able to transfer excitation energy between several PSII centers mediated by LHCIIs (connectivity), PSIIβ should not be connected [14]. Both our structural and biophysical data are summarized by a model of the supramolecular arrangement of PSII and LHCII in grana thylakoids.

2. Materials and methods

2.1. Preparation, unstacking and restacking of thylakoid membranes

Thylakoid membranes were isolated from 6 weeks old spinach leaves (*Spinacea oleracea* var. polka) grown hydroponically [15] at 13° to 16 °C according to [16]. The photoperiod (300 μmol quanta m^{-2} s^{-1}) was 10 h per day. Fresh isolated membranes were stored on ice in 330 mM sorbitol, 80 mM KCl, 7 mM $MgCl_2$ and 25 mM HEPES, pH 7.6, KOH. Unstacked thylakoids were prepared according to [17] with slight modifications. In detail, for unstacking thylakoids were adjusted to 2 mg Chl/mL and diluted 1:1 with buffer containing 5 mM KCl, 0.5 mM EDTA and 15 mM HEPES (pH 7.6) and incubated for 1 h on ice with slow stirring in darkness. The membranes were then diluted 1:50 with the same buffer and incubated for at least 30 min on ice (unstacking) followed by another 1:1 dilution using the same buffer. For restacking, unstacked membranes were 1:1 diluted in 160 mM KCl, 14 mM $MgCl_2$, 660 mM sorbitol and 35 mM HEPES (pH 7.6) and incubated for at least 1 h on ice. Stacked thylakoids were directly diluted in thylakoid buffer (see above) up to a Chl concentration of 10 μg/mL.

2.2. Spectroscopy

Chl *a* fluorescence induction curves were recorded in a laboratory built fluorometer according to [18] using the incubation buffer (see above). The Fo level was determined after 15 min incubation in strict darkness in the presence of 1 mM ferricyanide. The Fm level was deduced from a new sample in the presence of 1 mM sodium dithionite. In a separate experiment the fluorescence induction kinetics was recorded by adding 1 mM NH_2OH and 20 μM DCMU after 15-min incubation of the membranes in strict darkness. The kinetics was analyzed on the basis of the connected units model [14] according to [18].

For chlorophyll fluorescence spectra at 77 K, membranes were diluted in buffer medium (see above) at a Chl concentration of about 3 μM. 50 μL were applied on a filter paper (2 cm diameter) with a silver plate support and placed on the lucid bottom of a Dewar vessel. The Dewar was filled with liquid nitrogen. Light source was a halogen lamp in combination with the following optical filters: Schott BG18, Corning 9782 and LOT heat mirror filters producing a broad blue-green excitation (400 nm to 550 nm). Emission spectra were recorded with a Bausch and Lomb monochromator (1350 grooves/mm, 500 nm blaze) and a photomultiplier (Knott NL 2045-04-06) protected with a Schott RG630 filter. Typically, 25 spectra were averaged after correction for the spectral response of the set up.

2.3. Freeze-fracture electron microscopy

Freeze fracturing of stacked, unstacked and restacked thylakoids at −150 °C was performed with a BAF400T apparatus (Balzers, Lichtenstein). Platinum/carbon shadowing (45°), production of carbon replica and the conditions for the electron microscopy (EM208S, Philips, The Netherlands) are reported in detail in [8].

2.4. Analysis of EFs particle distributions

Next neighbor distribution functions (NNDF) and pair correlation function (PCF) were calculated from the Cartesian coordinates of the EFs particles in stacked, unstacked and restacked thylakoids as in [8]. For a given EFs particle, the NNDF quantify the probability to find the next neighbored particle at the indicated distance. The PCF quantifies the deviation of the local density at a distance r from a given particle from the global density (set as 1). Fig. 4A shows the distribution of nearest neighbor distances, indirectly indicating the NNDF.

3. Results

3.1. Unstacking and restacking of thylakoid membranes

Unstacking and restacking of unstacked grana thylakoids were examined by chlorophyll *a* fluorescence spectroscopy and freeze-fracture electron-microscopy. Fig. 1 shows examples of fluorescence induction curves (A) and low temperature emission spectra (B) of thylakoids incubated in buffers with different ionic strength to induce un- and restacking. Statistical analysis of the results deduced from these measurements is summarized in Table 1. Incubation in Mg^{2+}-free buffer in the presence of EDTA with a low concentration of monovalent cations ("unstacking" conditions) decreases the Fm / Fo ratio as well as the ratio of fluorescence emitted by PSII (F_{PSII}) *versus* PSI (F_{PSI}) at 77 K. These changes indicate a spillover of excitation energy from the PSII antenna system to the PSI antenna [19]. The rate constants for QA reduction (kα and kβ in Table 1) determined from the analysis of fluorescence induction curves (Fig. 1A) are proportional to the apparent antenna sizes of the PSIIα- and PSIIβ-centers [14]. In the unstacked state, the apparent antenna size of PSIIα and PSIIβ is decreased by 9% and 38%, respectively, as compared to stacked control membranes. Furthermore, the percentage of PSIIβ centers is increased and the connectivity parameter (J) for PSIIα decreased. Such low salt induced phenomena are well established (see e.g. refs [20,21]) and indicate an intermixing/randomization of the protein complexes associated with an unstacking of grana thylakoids [12]. In EM images of freeze-fractured thylakoids a change from the EF to the PF face or *vice versa* in the same membrane patch can only occur in stacked grana and not in unstacked membranes [22]. This was observed in thylakoids incubated under stacked and restacked conditions but rarely under low ionic strength conditions (not shown) indicating the predominance of unstacked grana thylakoids.

Table 1
Characterization of stacked, unstacked and restacked thylakoid membranes by Chl *a* fluorescence induction measurements and 77 K fluorescence emission spectra

	Stacked	Unstacked	Restacked	Significance stacked vs. restacked
Fm/Fo	5.05±0.19	2.02±0.02	4.86±0.08	−
PSIIβ fraction	45±1%	84±2%	47±2%	−
kα [a]	100±5%	91±2%	114±4%	+
kβ [a]	56±4%	35±2%	46±2%	+
J (connectivity)	1.7±0.2%	0.8±0.1%	1.1±0.1%	++
F_{PSII}/F_{PSI} at 77 K [b]	0.53±0.01	0.23±0.01	0.48±0.02	

Data represent the average of at least six independent measurements with standard deviation. Students significance test, error probability: −, not significant (α>40%); +, significant (α<5%); ++, highly significant (α<1%).
[a] The value of kα for stacked thylakoids (19.0±1 s^{-1}) was set to 100%.
[b] F_{PSII} is the average Chl fluorescence level between 682 and 694 nm and F_{PSI} at 735 nm.

Incubation of unstacked thylakoids in a buffer with high ionic strength for at least 1 h on ice results in an almost complete recovery of the Fm/Fo and the F_{PSII}/F_{PSI} ratios (Table 1), indicating resegregation of PSII and PSI due to restacking of the membranes [23]. This is supported by EM micrographs showing a change from one to the other fracture face in the same membrane patch (see above). Also, the Chl *a* fluorescence induction kinetics of restacked thylakoids is almost identical to stacked membranes (Fig. 1A). Mathematical analysis of these kinetics reveals a re-conversion of PSIIβ to PSIIα centers and an increase of the apparent PSIIα and PSIIβ antenna to almost the size of stacked control thylakoids (Table 1). Although there

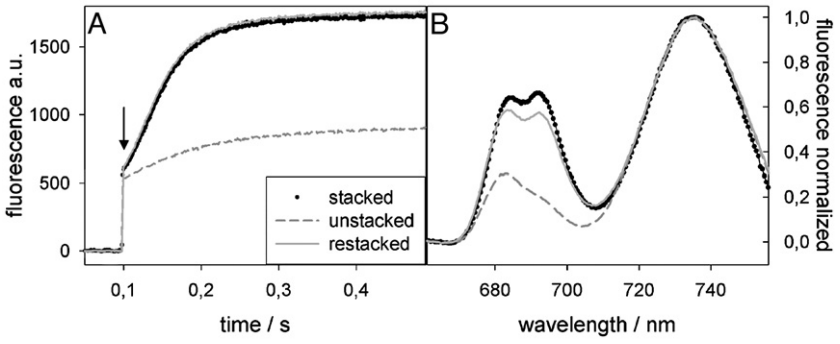

Fig. 1. Fluorescence analysis of thylakoids under stacking, unstacking and restacking conditions. (A) Chl *a* fluorescence induction kinetics in the presence of 20 μM DCMU at a Chl concentration of 10 μM. The induction kinetics was triggered by a fast shutter opening (opening time about 0.7 ms, indicated by an arrow) illuminating the dark-adapted sample with broad blue-green light (400 nm to 550 nm). (B) 77 K fluorescence emission spectra. Average of 25 scans for each spectrum with all spectra normalized to their maximal value after correction for wavelength dependence of the set-up.

is a slight increase (about 15%) in PSIIα and a reduction (about 10%) in PSIIβ antenna size in comparison to stacked control membranes, these results suggest that the segregation of the photosystems and the PSII antenna organization in restacked and stacked control thylakoids are nearly identical. In contrast, the connectivity parameter of PSIIα centers was reduced by about 30% in restacked membranes which is quite significant. This parameter quantifies the probability for an excitation energy migration among several PSII centers.

In summary, the fluorescence spectroscopic data in combination with the EM micrographs provide good evidence that the low salt treatment induces an unstacking of grana stacks and a randomization of the protein complexes, which is almost reverted under restacking conditions.

3.2. EF particle sizes in freeze-fractured thylakoids

To address the question whether unstacking leads to a monomerization of dimeric PSII complexes EF particle sizes in stacked and unstacked thylakoids were examined. There is good evidence that photosystem II complexes (monomeric and dimeric) are exclusively associated with the EF fracture face and all other protein complexes (LHCII, cyt b_6f, PSI, CFo) associated with the PF face [22]. Depending on their localization in stacked or unstacked membrane regions the EF particles are termed EFs and EFu [22]. To distinguish the EFs particle in restacked membranes from the stacked control membranes we use “EFrs” for “restacked conditions, stacked region”, and for EF particles in membranes prepared by unstacking we use “EFus” for “unstacked conditions”. Because in freeze fracture EM micrographs the lateral dimensions of monomeric PSII (6–12 nm) is significantly smaller than for dimeric PSII (10–20 nm), as shown for example by reconstitution studies of isolated complexes [22], the analysis of EF particle sizes could be a proper tool for investigating low salt induced monomerization of this photosystem. To check this possibility lateral dimensions of EFu und EFs particles were analyzed in stacked control thylakoids. Due to the fact that EF particles have an elliptical shape [22] EFs and EFu particles in stacked control thylakoids were fitted with an ellipse using a particle count routine (Optimas program version 6.5.). Fig. 2A to D shows the size distributions of ellipses long axis and width for both types of EF areas deduced from fitting. Table 2 summarized the lateral dimension extracted from these histograms. The sizes of the long axis as well as the width are clearly distinguishable between EFs (Fig. 2A, B) and EFu (Fig. 2C, D) particles. The dimensions of about 16.0 × 9.6 nm (EFs) and 10.5 × 6.5 nm (Table 2) fit in the range of published data [22]. In the literature good evidence exists that EFu objects represent monomeric PSII and EFs particles dimeric PSII [22,24]. Therefore the size distributions in Fig. 2A to D and the numbers in Table 2 can be used to analyze whether unstacking of thylakoids leads to a monomerization of dimeric PSII complexes or to other changes in the PSII size.

Due to the fact that unstacking of thylakoids is accompanied by an abolishment of stacked and unstacked thylakoid regions (see above) only one EF fracture face is apparent in these

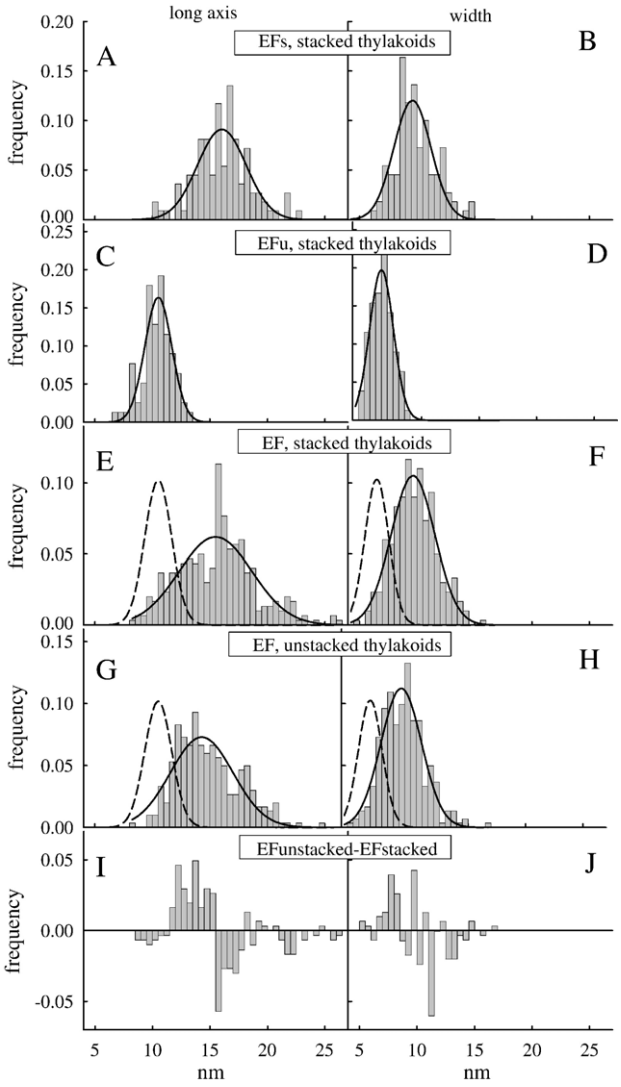

Fig. 2. Size analysis of EF particles. EF particles in freeze fractured micrographs of stacked and unstacked thylakoid membranes were fitted with an ellipse. The deduced values for the long axis (A, C, E, G) and width (B, D, F, H) are shown. (A, B) EFs particles and C, D, EFu particles from stacked control thylakoids. (E, F) EF particles from stacked thylakoids without differentiation in EFs and EFu. (G, H) from unstacked membranes. The histograms were fitted with Gaussian curves (bold lines). The results of this fitting are summarized in Table 2. Dashed lines in panels E to H show the gauss curves for EFu particles (C and D), respectively. Panels I and J give the difference of unstacked minus stacked thylakoids. Number of analyzed EF particles: A and B, 111; C and D, 78; E and F, 300; G and H, 302.

membranes. For a better comparison between EF particle sizes from unstacked thylakoids with stacked control membranes, particle size analysis without differentiation in EFs and EFu areas was conducted for the latter (Fig. 2E and F), i.e. EF particles from stacked thylakoids were randomly selected from EFs and EFu areas. As expected the histograms for the long axis (Fig. 2E) and the width (Fig. 2F) are broadened compared to Fig. 2A to D due to a mixing of EFs and EFu particles (see also Table 2). The lateral dimensions of about 15.5 × 9.7 nm are more similar to EFs and not to EFu objects (Table 2) indicating that dimeric PSII dominate in stacked thylakoids as was confirmed by electron microscopic and biochemical analysis (e.g., [3,22]).

Table 2
Long axis and width of EF particles from stacked and unstacked thylakoids

	EFs stacked thylakoids	EFu stacked thylakoids	EF stacked thylakoids	EF unstacked thylakoids	EF restacked thylakoids
Long axis	16.0±2.1 nm	10.5±1.2 nm	15.5±3.2 nm	14.3±2.7 nm	14.5±3.2 nm
Width	9.6±1.6 nm	6.5±1.0 nm	9.7±1.9 nm	9.2±1.8 nm	8.7±1.4 nm

Values represent the results of fitting the size histograms in with gauss functions. Values for restacked thylakoids were derived from not shown histograms. ±values give the width of the gauss curves.

The size histograms of unstacked thylakoids reveal a small reduction in the long axis and a still lesser decreased width (Fig. 2G and H) compared to their counterparts from stacked membranes (Table 2). Clearly no significant shift to lateral values corresponding to monomeric EFu particles is apparent in unstacked thylakoids (compare dashed lines with the histogram in Fig. 2G and H and Table 2). This gives strong evidence that incubating thylakoids in low salt media for unstacking did not induce a significant monomerization of dimeric PSII complexes. Although the data indicate that PSII monomer/dimer ratio is unchanged in unstacked membranes the lateral dimensions are smaller compared to particles from stacked membranes. To analyze the reduction in the EF particle size a difference plot (unstacked minus stacked) was calculated (Fig. 2I and J). For the long axis sizes peaking around 13.5 nm are more abundant and sizes around 17 nm less frequent in thylakoids incubated under unstacking conditions (Fig. 2I). Concerning the width of the ellipses the data are less clear (Fig. 2J). There is a tendency of a reduction in width from about 11.5 to 8.5 nm. Overall the EF particles size analysis of unstacked thylakoids give good evidence that dimeric PSII complexes are not converted to monomers. Furthermore a size reduction for a fraction of the EF particles of about 3.5 nm in length and about 3 nm in width was observed (Fig. 2).

3.3. EFs particle distribution analysis in stacked, unstacked and restacked thylakoids

In order to examine the PSII arrangement in thylakoid membranes on a supramolecular level, the x- and y-positions of the EFs, EFus and EFrs particles were analyzed (for example, see Fig. 3) by NNDF and PCF. Results of this analysis are shown in Fig. 4A and B. The EF particle densities for stacked, unstacked and restacked thylakoids are 1848±383 μm^{-2}, 1529±385 μm^{-2} and 1747±254 μm^{-2}, respectively. From the values of Fig. 4A, we calculated a mean distance to the next neighbored EFs particle of about 20 nm (from center to center), which is in accordance with our previous study for stacked grana [8] and reflects the high protein density: The mean distance between two neighbored photosystems is similar to the dimension of the PSII–LHCII supercomplex of about 27×12 nm [25].

In the next neighbor distribution of the EFs and EFus particles, significant differences are apparent (Fig. 4A, left), especially a broadening of the bell-shaped distribution upon unstacking: The half width increases from 9.1 nm for the EFs to 13.4 nm for EFus. This broadening indicates a randomization of the particle distribution in unstacked thylakoids [13] which is in agreement with the spectroscopic data (see above). *Vice versa* the narrowing of the next neighbor distribution for stacked

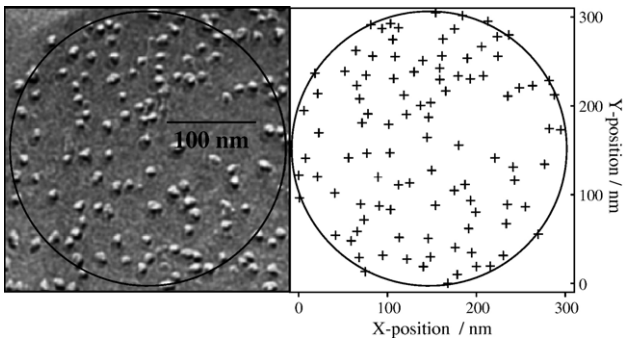

Fig. 3. Typical electron micrograph of a freeze fractured thylakoid membrane prepared by unstacking (left) and the positions of the EF particles as determined from the micrograph (right). The EM image shows an EF fracture face, which is clearly distinguishable from the PF face due to the fact that the EF face contains significant larger and less dense packed particles. Circles indicate the region used for the particle analysis in Fig. 4. The particle density is 1380 μm^{-2}.

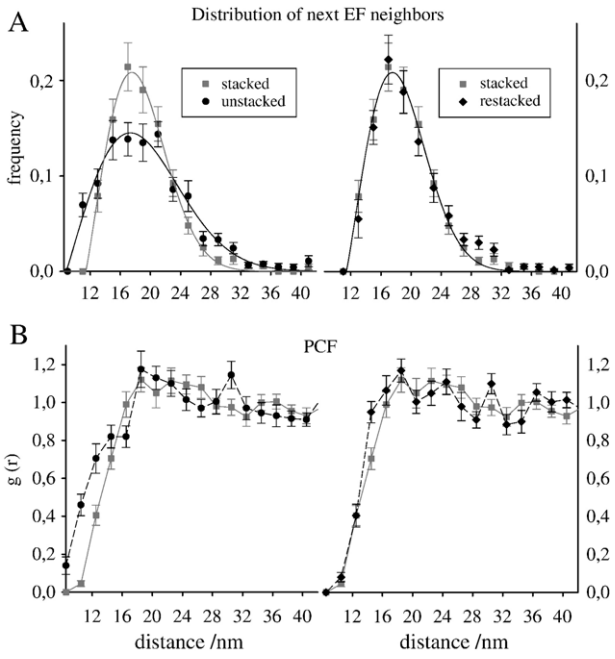

Fig. 4. NNDF (5A) and PCF (5B) analysis of EF particles in stacked, unstacked and restacked thylakoids. (A) 18 EM images (806 particles) from stacked, 14 images (565 particles) from restacked and 15 images (774 particles) from unstacked thylakoids were analyzed and averaged. The error bars indicate the standard error of the mean value. The data were fitted (grey and black lines) with an asymmetric bell-shaped curve (4 parameter Weibull) to deduce the half width. (B) The PCF quantifies the deviation of the local density relative to the global density as a function of the distance to a typical particle. The same data set as for the NNDF was used.

control membranes compared with the (randomized) unstacked thylakoids suggests an even more ordered PSII arrangement in grana stacks as was recently postulated [8]. In detail, distances around 11 nm and between 25 and 30 nm are less frequent and distances between 17 and 20 nm are more frequent in stacked grana (Fig. 4A, left). The depopulation of shorter and longer distances under stacked conditions indicates the existence of repulsive as well as attractive forces between PSII complexes. A less pronounced but nonetheless significant difference is also visible in the PCF analysis (Fig. 4B, left). In particular, in unstacked thylakoids the local EFs density at shorter distances (8 to 11 nm) is higher than in stacked control thylakoids, which is in accordance with the results of the NNDF analysis.

Within the range of error, restacking of unstacked thylakoids leads to a rearrangement of the EFs particle distribution, which is almost indistinguishable from stacked control membranes (Fig. 4A and B right panels). Although there are small differences in the PCF at the distances between 15 and 31 nm, the combined results of both analyses strongly suggest that the EFs distributions of restacked and stacked control membranes are identical.

4. Discussion

4.1. Unstacking of grana thylakoids

The unstacking of thylakoid membranes is a complex process. Staehelin distinguished three steps upon incubating isolated thylakoids in low ionic strength buffers [12]: (i) rapid separation of appressed regions, (ii) increase in the tubular diameter of the connections between grana and stroma lamellae associated with intermixing of the protein complexes and (iii) complete unfolding of grana and reorganization of the protein complexes. It is likely that the lateral reorganization of the protein complexes is followed by and a consequence of the unstacking of grana [26]. Fluorescence data (Fm / Fo and F_{PSII}/F_{PSI}) (see Table 1) and particle distribution analysis (Fig. 4A and B, left panel) indicates that step (ii) is realized under our unstacking conditions. Also, the freeze-fracture micrographs under unstacked conditions suggest that the grana are almost completely unstacked (step iii). Moreover, our data strongly indicate an intermixing and randomization of the proteins (especially PSII, LHCII and PSI) under unstacked conditions. These low-salt induced alterations can be explained by an increased electrostatic repulsion of negative thylakoid surface charges which is accompanied by the unstacking of the grana [27].

EF particle size analysis (Fig. 2, Table 2) give clear evidence that incubation of thylakoids in low salt buffer for unstacking did not induce significant conversion of dimeric PSII complexes into the monomeric form. This is in good accordance with observations that the dimeric organization of PSII is not effected by a low salt-treatment in isolated LHCII–PSII supercomplexes [28] or in intact thylakoids [24]. On the other hand, the analysis of the fluorescence induction curves reveals a conversion of PSIIα into PSIIβ centers. As PSIIβ centers are assumed to be monomeric and have a 2 to 3 times smaller antenna size than PSIIα [29], it appears, that structural dimers are functionally monomers under unstacked conditions. Noteworthy, under unstacked conditions the Fv level is lower due to energy spillover from PSII to PSI (see Fm / Fo in Table 1 and Fig. 1) and the sigmoidicity of fluorescence induction curves of isolated PSII dimers indicating connectivity is low [30] and therefore difficult to detect. For this reason, functional isolated dimers with low connectivity, which are hardly distinguishable from PSIIβ centers, may exist under unstacked conditions. In order to test this possibility we repeated our mathematical analysis assuming that the fraction of PSIIβ centers (45% to 47%, Table 1) is unchanged in unstacked thylakoids compared to stacked and restacked membranes. Using a value of 46% the calculation resulted in a connectivity parameter for PSIIα of 0.2 ± 0.1 (not shown). The mean quadratic deviation between theoretical and measured fluorescence induction data is 0.20×10^{-3}, assuming that the PSIIβ-fraction is identical to the stacked thylakoids, and 0.17×10^{-3} with a free running fit for the β-fraction. In conclusion, the induction curves from unstacked thylakoids can be reasonably fitted by a model which assumes an identical number of (dimeric) PSIIα centers under stacked and unstacked conditions with low connectivity. This indicates the possibility that isolated excitonic coupled PSII dimers could exist in unstacked thylakoids, which is supported by an observation that incubation of thylakoids in Mg^{2+} free media does not abolish the α/β heterogeneity but leads to a selective change in the PSIIα characteristics [31]. Furthermore isolated PSII dimers from cyanobacteria have a connectivity parameter of 0.3 whereas isolated monomers show no connectivity (M. Rögner, unpublished results). This is in accordance with our suggestion that in unstacked thylakoids isolated PSII dimers with a low connectivity may exist. The low connectivity value of isolated dimers has the interesting consequence that the main part of the excitonic coupling of PSII in grana stacks ($J = 1.7$, Table 1) must come from the interaction of several dimers mediated probably via LHCII. On the other hand, analysis of the fluorescence induction curves provided clear evidence for a drastic decreased antenna size of PSII centers in unstacked membranes. The mean rate constant of QA reduction (averaging α and β centers) decreased to about 55% compared to stacked control thylakoids (calculated from Table 1). Considering that LHCII-trimers contain about 50% of all chlorophylls connected to PSII [5] this indicates a disconnection of LHCII trimers from PSII centers. An additional disconnection of all minor LHCII subunits from the PSII-core is unlikely because the antenna size would decrease to less than 20% (assuming 35 chlorophylls for the D1/D2/CP43/CP47 complex) in contrast to the measured 55%. The EF particle size analysis suggests that a mass of about 3.5×3 nm is removed from PSII under unstacked conditions (Fig. 2I and J). This size corresponds roughly to a monomeric LHCII subunit [32]. Thus it is likely that in addition to major trimeric LHCII one minor momomeric LHCII unbinds from PSII in the course of unstacking but that the other minor LHCII complexes are still bound. It appears that the low-salt treatment induces only a partial disruption of the LHCII–PSII supercomplex. Obviously, the lateral electrostatic repulsion of

negative surface charges on the protein subunits which dominate under unstacked conditions [27] are strong enough to separate LHCII-trimers (and probably one minor LHCII) from PSII but are too weak to disperse the remaining subunits. This indicates a hierarchy of protein interactions in PSIIα centers. The binding affinity of the major trimeric LHCII to the PSII-core complex could be lower than that of the minor LHCII subunits. In addition to the reduction in the PSII antenna size, the connectivity parameter decreases indicating the separation of PSIIα centers. The upper part of the model shown in Fig. 5 summarizes these findings. The functional consequence of the altered PSII organization in unstacked thylakoids is a significant decrease in the photochemical quantum efficiency of PSII [19] from 0.80 (stacked control membranes) to 0.50 (unstacked conditions, as determined from the Fm / Fo ratio in Table 1).

An interesting observation is that a fraction of EFus particles are in closer contact (distances between 10 and 12 nm, see Fig. 5) than in the stacked control membranes. This is quite unexpected as the membrane lipid area is even increased in thylakoids under unstacked conditions due to the intermixing with stroma lamellae and grana margins, which have a lower protein density. Also, an intermixing with proteins from the unstacked regions (PSI, ATPase) should rather increase the EF separation. Indeed, the overall EFus density is decreased in comparison with stacked thylakoids by about 15%. The phenomenon of approaching PSII complexes can also be observed in our computer simulations, if no interaction between protein complexes is assumed, i.e. in a pure random arrangement [8]. This is simply a statistical consequence and can be explained by direct contact of adjacent PSII–dimer complexes in the membrane plane. As pointed out earlier, the problem of a direct PSII-dimer–PSII-dimer contact is that the Q_B binding pocket for plastoquinone can be blocked hindering an efficient electron transfer from PSII to the PQ-pool [8]. Obviously, in stacked membranes the direct PSII–PSII contact is avoided (Fig. 4A and B) by specific LHCII binding sites on PSII [33]. Due to the fact that LHCII disconnects under low salt conditions from PSII (see above) it is likely that these interactions are mainly electrostatically stabilized [27]. These findings point to the significance of salt induced specific interactions between PSII and LHCII for an efficient electron transfer in grana thylakoids.

4.2. Self organization of PSII in grana thylakoids

As discussed above, incubating thylakoids under unstacking conditions leads to intermixing and randomization of the protein complexes, accompanied by disconnection of LHCII trimers

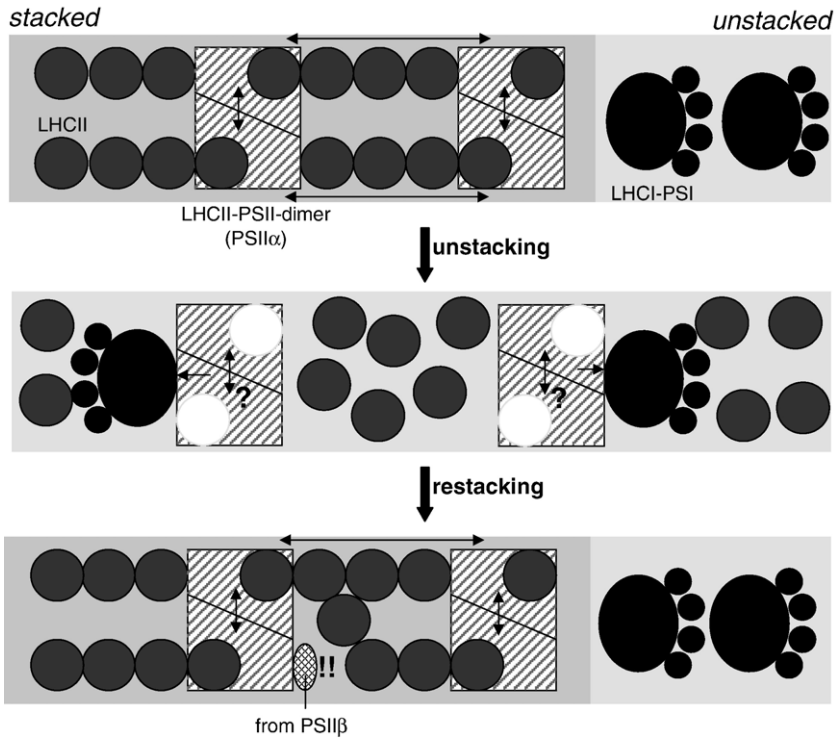

Fig. 5. Model illustrating the changes in the protein organization upon unstacking and restacking of thylakoid membranes. The model focuses on the PSII–LHCII supercomplex organization (probably PSIIα centers). Upper part: In the mean PSII supercomplex are connected with about 4 LHCII-trimers under stacked conditions, are excitonically coupled (connectivity) and are well separated from PSI in unstacked regions. Middle part: Unstacking leads to randomization of the protein arrangement and the separation of LHCII-trimers from PSII. PSI and PSII come in excitonic contact (spillover). Our data indicate that the low-salt treatment does not result in a structural monomerization of PSII-dimers. The functional monomerization, i.e. whether the dimers are excitonically uncoupled under these conditions, is still unclear as symbolized by the question mark (see text for details). The white circles at the PSII supercomplexes indicate unoccupied binding sites for LHCII-trimers. Lower part: restacking of unstacked thylakoids leads to almost the same macromolecular organization as in untreated membranes, i.e. rebinding of LHCII-trimers to PSII and a resegregation of PSII and PSI. We propose a redistribution of minor LHCIIs from PSIIβ centers to PSIIα, where they may bind to one of the LHCII-trimer binding sites (exclamation point). This may result in a decreased connectivity between PSIIα centers.

from PSII and a decreased connectivity between PSIIα centers. Starting from this randomized arrangement, re-addition of mono- and divalent cations induces a restacking of grana and resegregation of the protein complexes. This rearrangement is time dependent [12]. According to our data, a 1-h incubation time is sufficient to ensure a maximal recovery of the fluorescence parameter presented in Table 1. The EFrs particle analysis of restacked membranes (Fig. 4) shows no significant differences to stacked control membranes, at least at the resolution of the EM micrographs of freeze-fracture thylakoids, indicating an identical PSII arrangement. These data provide good evidence that the spatial separation of PSI and PSII on unstacked and stacked membrane regions and the formation of PSIIα- from PSIIβ-centers as well as the macromolecular organization of PSII in stacked grana thylakoids is a self-organizing process. Thus, these processes are determined by the physicochemical and structural properties of the protein complexes themselves and are induced by a certain ionic milieu. Since thylakoids are very dynamic membranes which respond to changes in the environmental conditions by rearrangements of their protein organization (e.g. state transitions [34], PSII repair cycle [11] or long term adaptations [22]) the self-organization could be an important feature for the maintenance of the functional integrity of the photosynthetic machinery. Regarding the biogenesis of PSII supercomplexes it is important to recognize that our Mg^{2+} depletion experiments do not induce a complete disassembly of the supercomplexes. As discussed above the low salt treatment leads to disconnection of LHCII trimers and probably one minor LHCII while leaving the remaining dimeric PSII complexes (PSII core plus minor LHCII) intact. Starting from this complex the formation of the macromolecular network of PSII and trimeric LHCII in stacked grana thylakoids is self-organized. The structural basis for this could be the specific LHCII-trimer binding sites on PSII [33,35] or specific lipids surrounding the proteins, i.e. a hydrophobic recognition as found for lipid rafts [36]. Recently, a molecular model for the stacking of grana thylakoids based on the charge distribution on the flat stromal surface of LHCII trimers was presented [32]. According to this model the intermolecular attraction between LHCIIs in opposite membranes is the result of a sophisticated balance between electrostatic attraction and repulsion of positively and negatively charged protein regions. This balance is strongly influenced by screening effects of cations, namely Mg^{2+} ions. It is likely that similar forces are also involved in the lateral organization of the protein complexes in grana membranes. In addition, there is evidence that these pure protein–protein interactions are modulated by specific lipid–protein interactions [37,38].

However, a closer look reveals subtle differences between stacked and restacked thylakoid membranes. The antenna size of PSIIα centers is slightly but significantly increased which is accompanied by a decrease of the connectivity parameter *J* and a decrease in the PSIIβ antenna size (Table 1). The most likely explanation for this difference in the antenna size is a redistribution of LHCII subunits from β to α centers in the course of restacking. Assuming that, at the average, a PSIIα center in stacked control membranes is associated with about 230 chlorophylls [5], PSIIα in restacked membranes should bind 34±23 more chlorophylls (calculated from kα in Table 1, taking the standard deviations into account). For the PSIIβ centers the antenna size under restacked conditions is reduced by 28±9 chlorophylls. These calculations suggest that two to four minor or major monomeric LHCII subunits are redistributed from PSIIβ to PSIIα centers. Noteworthy no increase in the EFrs size was detected compared to EF (stacked) particle (Table 2). This could indicate that the extra chlorophylls associated with PSIIα complexes in restacked membranes came from trimeric LHCII because this complex is associated with the PF fracture face. However, the significance of the differences in sizes in Table 2 is weak (see standard deviations). Therefore no definite answer is possible at this point. The changes in the antenna size of PSIIα are accompanied by a decreased connectivity. Our interpretation for this phenomenon is depicted in the lower part of Fig. 5: Starting from unstacked membranes in which minor LHCII complexes are released from PSIIβ, these subunits have a certain probability to bind to one (or more) LHCII-trimer binding sites on the PSIIα supercomplex [33] in the course of restacking. There is evidence that there are three distinct binding sites on the PSII complexes in grana thylakoids which have different binding strength called *S* (strong), *M* (moderate) and *L* (loose) [33,35]. The structural data of these PSII–LHCII supercomplexes suggests that the LHCII-trimer binding on the *S* and *M* site is facilitated by a combination of two of the minor antenna complexes (CP24 and CP29 or CP26 and CP29). Thus it is likely that the strength of the binding depends on the number of minor LHCII subunits acting as docking partners. We assume that the additional LHCII subunits from PSIIβ interact with these minor LHCII from PSIIα, which results in the occupation of the *S*, *M* or *L* site. As a consequence only one instead of two minor LHCII on PSIIα acts as a docking site for trimeric LHCII leading to decreased binding strength and an impaired excitonic interaction between LHCII trimers and PSII subunit. An alternative explanation is that part of the so-called C2S2M2 megacomplex [6], consisting of a PSII dimer (C2), two strongly (S2) and two moderately (M2) bound LHCII-trimers is not at all reformed. There are indications that this megacomplex is the building block in grana thylakoids [6]. However, these proposed subtle changes have almost no effect on the photochemical quantum efficiency: from Table 1 we calculate a value of 0.79 for restacked membranes, which is virtually the same as for stacked control thylakoids.

In summary, our data gave evidence that low salt induced electrostatic repulsion leads to a lateral separation of LHCII-trimer from the PSII-core, however leaving the core-dimer intact. This indicates a hierarchy of protein–protein interactions for the stability of the PSII–LHCII associations in grana thylakoids. The restacking results show that the specificity of LHCII-binding sites play a key role in the organization of the protein arrangement in grana thylakoids.

Acknowledgements

The authors acknowledge the financial support from the Deutsche Forschungsgemeinschaft (H.K. and S.H. by HK818/

2-2, 3-1 and 4-1 and T.J. and M.R. by SFB 480, project C1) and the critical proof reading by Dr. G. Bernat.

References

[1] L. Mustardy, G. Garab, Granum revisited. A three-dimensional model—Where things fall into place, Trends Plant Sci. 8 (2003) 117–122.

[2] P.-A. Albertsson, A quantitative model of the domain structure of the photosynthetic membrane, Trends Plant Sci. 6 (2001) 349–354.

[3] R. Danielsson, P.-A. Albertsson, F. Mamedov, S. Styring, Quantification of photosystem I and II in different parts of the thylakoid membrane from spinach, Biochim. Biophys. Acta 1608 (2004) 53–61.

[4] A. Rokka, M. Suorsa, A. Saleem, N. Battchikova, E.-M. Aro, Synthesis and assembly of thylakoid protein complexes: multiple assembly steps of photosystem II, Biochem. J. 388 (2005) 159–168.

[5] B. Hankamer, J. Barber, E.J. Boekema, Structure and membrane organization of photosystem II in green plants, Annu. Rev. Plant Physiol. Plant Mol. Biol. 48 (1997) 641–671.

[6] J.P. Dekker, E.J. Boekema, Supramolecular organization of thylakoid membrane proteins in green plants, Biochim. Biophys. Acta 1706 (2005) 12–39.

[7] M. Rögner, E.J. Boekema, J. Barber, How does photosystem 2 split water? The structural basis of efficient energy conversion, Trends Biochem. Sci. 21 (1996) 44–49.

[8] H. Kirchhoff, I. Tremmel, W. Haase, U. Kubitscheck, Supramolecular photosystem II organization in grana thylakoid membranes: Evidence for a structured arrangement, Biochemistry 43 (2004) 9204–9213.

[9] E. Baena-Gonzalez, E.-M. Aro, Biogenesis, assembly and turnover of photosystem II units, Philos. Trans. R. Soc. London, B 357 (2002) 1451–1460.

[10] P. Nixon, M. Barker, M. Boehm, R. de Vries, J. Komenda, FtsH-mediated repair of the photosystem II complex in response to light stress, J. Exp. Bot. 56 (2004) 357–363.

[11] B. Andersson, E.-M. Aro, Photodamage and D1 protein turnover in photosystem II, in: E.-M. Aro, B. Andersson (Eds.), Regulation in photosynthesis, Kluwer Academic Publishers, Dordrecht, The Netherlands, 2001, pp. 377–393.

[12] L.A. Staehelin, Chloroplast structure and supramolecular organization of photosynthetic membranes, in: L.A. Staehelin, C.J. Arntzen (Eds.), Photosynthesis III: Photosynthetic membranes and light-harvesting systems, Springer-Verlag, Berlin, Germany, 1986, pp. 1–84.

[13] U. Kubitscheck, R. Peters, Localization of single nuclear pore complexes by confocal scanning microscopy and analysis of their distribution, Methods Cell Biol. 53 (1998) 79–98.

[14] J. Lavergne, H.-W. Trissl, Theory of fluorescence induction in photosystem II: derivation of analytical expressions in a model including exciton-radical-pair equilibrium and restricted energy transfer between photosynthetic units, Biophys. J. 68 (1995) 2474–2492.

[15] P.J. Randall, D. Bouma, Zinc deficiency, carbonic anhydrase, and photosynthesis in leaves of spinach, Plant Physiol. 52 (1973) 229–232.

[16] H. Kirchhoff, S. Horstmann, E. Weis, Control of the photosynthetic electron transport by PQ diffusion microdomains in thylakoids of higher plants, Biochim. Biophys. Acta 1459 (2000) 148–168.

[17] C. Enz, T. Steinkamp, R. Wagner, Ion channels in the thylakoid membrane (a patch-clamp study), Biochim. Biophys. Acta 1143 (1993) 67–76.

[18] H. Kirchhoff, M. Borinski, S. Lenhert, L. Chi, C. Büchel, Transversal and lateral exciton energy transfer in grana thylakoids of spinach, Biochemistry 43 (2004) 14508–14516.

[19] G.H. Krause, E. Weis, Chlorophyll fluorescence and photosynthesis: The basics, Annu. Rev. Plant Physiol. Plant Physiol. Mol. Biol. 42 (1991) 313–349.

[20] J.-M. Briantais, C. Vernotte, J. Olive, F.-A. Wollman, Kinetics of cation-induced changes of photosystem II fluorescence and of lateral distribution of the two photosystems in the thylakoid membranes of pea chloroplasts, Biochim. Biophys. Acta 766 (1984) 1–8.

[21] B.-D. Hsu, J.-Y. Lee, A study on the fluorescence induction curve of the DCMU-poised chloroplast, Biochim. Biophys. Acta 1056 (1991) 285–292.

[22] L.A. Staehelin, G.W.M. van der Staay, Structure, composition, functional organization and dynamic properties of thylakoid membranes, in: D.A. Ort, C.F. Yocum (Eds.), Oxygenic photosynthesis: The light reactions, Kluwer Academic Publishers, Dordrecht, Netherlands, 1996.

[23] L.A. Staehelin, Reversible particle movements associated with unstacking and restacking of chloroplast membranes in vitro, J. Cell Biol. 71 (1976) 136–158.

[24] J. Dekker, M. Germano, H. van Roon, E.J. Boekema, Photosystem II solubilizes as a monomer by mild detergent treatment of unstacked thylakoid membranes, Photosynth. Res. 72 (2002) 203–210.

[25] J. Nield, E.V. Orlova, E.P. Morris, B. Gowen, M. van Heel, J. Barber, 3D map of the plant photosystem II supercomplex obtained by cryoelectron microscopy and single particle analysis, Nat. Struct. Biol. 7 (2000) 44–47.

[26] G. Garab, L. Mustardy, Role of LHCII-containing macrodomains in the structure, function and dynamics of grana, Aust. J. Plant Physiol. 26 (1999) 649–658.

[27] J. Barber, Influence of surface charges on thylakoid structure and function, Annu. Rev. Plant Physiol. 33 (1982) 261–295.

[28] R. Harrer, Associations between light-harvesting complexes and photosystem II from *Marchantia polymorpha* L. determined by two- and three-dimensional electron microscopy, Photosynth. Res. 75 (2003) 249–258.

[29] J. Lavergne, J.-M. Briantais, Photosystem II heterogeneity, in: D.A. Ort, C.F. Yocum (Eds.), Oxygenic photosynthesis: The light reactions, Kluwer Academic Publishers, Dordrecht, The Netherlands, 1996, pp. 265–287.

[30] P. Jahns, H.-W. Trissl, Indications for a dimeric organization of the antenna-depleted reaction center core photosystem II in thylakoids of intermittent light grown pea plants, Biochim. Biophys. Acta 1318 (1997) 1–5.

[31] A. Melis, P.H. Homann, A selective effect of Mg^{2+} on the photochemistry at one type of reaction center in photosystem II of chloroplasts, Arch. Biochem. Biophys. 190 (1978) 523–530.

[32] J. Standfuss, V.A. Terwisscha, M. Lamborghini, W. Kühlbrandt, Mechanisms of photoprotection and nonphotochemical quenching in pea light-harvesting complex at 2.5 A resolution, EMBO J. 24 (2005) 919–928.

[33] E.J. Boekema, F. Calkoen, R. Bassi, J.P. Dekker, Multiple types of association of photosystem II and its light-harvesting antenna in partially solubilized photosystem II membranes, Biochemistry 38 (1999) 2233–2239.

[34] J.F. Allen, State transitions—A question of balance, Science 299 (2003) 1530–1532.

[35] A.E. Yakushevska, P.E. Jensen, W. Keegstra, H.V. Scheller, E.J. Boekema, J.P. Dekker, Supermolecular organization of photosystem II and its associated light-harvesting antenna in *Arabidopsis thaliana*, Eur. J. Biochem. 268 (2001) 6020–6028.

[36] S. Munro, Lipid rafts: Elusive of illusive? Cell 115 (2003) 377–388.

[37] S. Nußberger, K. Dörr, D.N. Wang, W. Kühlbrandt, Lipid–protein interactions in crystals of plant light-harvesting complex, J. Mol. Biol. 234 (1993) 347–356.

[38] I. Simidjiev, S. Stoylova, H. Amenitsch, T. Jávorfi, L. Mustárdy, P. Laggner, A. Holzenburg, G. Garab, Self-assembly of large, ordered lamellae from non-bilayer lipids and integral membrane proteins in vitro, Proc. Natl. Acad. Sci. 97 (2000) 1473–1476.